International Symposium
On Turbulence and Shear Flow
Phenomena (TSFP-9)
June 30 - July 3, 2015 *Melbourne, Australia*

INFLUENCE OF GRAVITATIONAL SETTLING ON TURBULENT DROPLET CLUSTERING AND RADAR REFLECTIVITY FACTOR

Keigo Matsuda, Ryo Onishi, Keiko Takahashi
Center for Earth Information Science and Technology
Japan Agency for Marine-Earth Science and Technology (JAMSTEC)
3173-25 Showa-mach, Kanazawa-ku, Yokohama 236-0001, Japan
k.matsuda@jamstec.go.jp, onishi.ryo@jamstec.go.jp, takahasi@jamstec.go.jp

ABSTRACT

For radar cloud observations, the microwave refectivity of clouds is measured as the radar reflectivity factor Z, which is dependent on the cloud microphysical properties. Previous study has clarified that turbulent droplet clustering can be a cause of significant increase of the radar reflectivity factor. However, the influence of gravitational settling still remains to be clarified. This study, thus, investigates the influence of gravitational settling on the spatial distribution of turbulent clustering droplets and the radar reflectivity factor. A three-dimensional direct numerical simulation (DNS) of particle-laden isotropic turbulence is conducted for several values of the nondimensional terminal velocity S_v. The results show that the power spectrum of droplet number density fluctuation, which is calculated from the DNS data, depends on S_v: as the droplet settling becomes stronger, the spectrum increases at small wavenumbers and decreases at large wavenumbers. The radar reflectivity factor Z is estimated from the power spectrum under ideal cloud conditions. The results indicate that the influence of turbulent clustering is suppressed under strong gravitational-settling conditions.

INTRODUCTION

A large number of radar observations have been conducted to improve our understanding of cloud physics (Stephens *et al.*, 2008; Okamoto *et al.*, 2007). In the radar observation, microwave is transmitted from an antenna toward a target cloud and the reflected microwave is received and analyzed. The relation between the transmitted microwave power P_t and the received microwave power P_r are given by the following radar equation:

$$P_\mathrm{r} = \frac{P_\mathrm{t} G^2 k_\mathrm{m}^2 |K|^2 V}{4^5 R^4} Z, \tag{1}$$

where G is the antenna gain, k_m the microwave wavenumber, K the dielectric coefficient, R the distance between the antenna and the clouds, and Z the radar reflectivity factor, which is dependent on the cloud microphysical properties. This implies that cloud properties can be estimated from Z under some assumptions: randomness and uniformity of droplet distribution are usually assumed. In contrast, cloud turbulence forms nonuniform spatial distribution of droplets, which is referred to as turbulent clustering of droplets (Maxey, 1987; Squires & Eaton, 1991; Chen *et al.*, 2006). There have been several studies reporting that the radar reflectivity factor Z of clustering particles is larger than that of randomly-dispersed particles (Kostinski & Jameson, 2000; Erkelens *et al.*, 2001). The increment is attributed to the coherent microwave scattering and depends on the power spectrum of droplet number density fluctuations $E_\mathrm{np}(k)$ (Erkelens *et al.*, 2001). Recently, Matsuda *et al.* (2014) have performed a three-dimensional direct numerical simulation (DNS) to obtain turbulent droplet clustering data and revealed that the influence of turbulent clustering can be a cause of significant observational errors. In order to analyze the influence more accurately, however, it is necessary to clarify the influence of gravitational settling. This study aims to clarify the influence of gravitational settling on the spatial distribution of turbulent clustering droplets and the radar reflectivity factor by means of a three-dimensional DNS of particle-laden isotropic turbulence.

COMPUTATIONAL METHOD

Air Turbulence

Governing equations of the turbulent air flow are the continuity and Navier-Stokes equations for three-dimensional incompressible flows:

$$\frac{\partial u_i}{\partial x_i} = 0, \tag{2}$$

$$\frac{\partial u_i}{\partial t} + \frac{\partial u_i u_j}{\partial x_j} = -\frac{1}{\rho_\mathrm{g}} \frac{\partial p}{\partial x_i} + \nu \frac{\partial^2 u_i}{\partial x_j \partial x_j} + F_i, \tag{3}$$

where u_i is the air velocity in ith direction, p the pressure, ρ_g the density of air, ν the kinematic viscosity and F_i the external force in ith direction. The fourth-order central difference scheme is used for the advection term and the second-order Runge-Kutta scheme for time integration. The velocity and pressure are coupled by the highly simplified marker and cell (HSMAC) method. Statistically steady turbulence is generated by applying the Reduced Communication Forcing (RCF) (Onishi *et al.*, 2011), which maintains the intensity of large-scale eddies keeping high parallel efficiency, to the external force F_i.

Droplet Motions

Droplet motions are tracked by the Lagrangian method. The governing equation is

$$\frac{dv_i}{dt} = -\frac{v_i - u_i}{\tau_\mathrm{p}} + g_i, \tag{4}$$

where v_i is the droplet velocity in ith direction, τ_p the droplet relaxation time and g_i the gravitational acceleration in ith direction. Droplets are assumed as Stokes particles, whose relaxation time τ_p is given as

$$\tau_\mathrm{p} = \frac{\rho_\mathrm{p}}{\rho_\mathrm{g}} \frac{d_\mathrm{p}^2}{18\nu}, \tag{5}$$

where ρ_p is the density of water and d_p the droplet diameter. The gravitational acceleration is applied in $-x$ direction. Turbulence modulation and collisions between droplets are neglected since cloud droplets are typically dilute enough.

Computational conditions

The computational domain is set to a cube with edge length of $2\pi L_0$, where L_0 is the representative length scale. Periodic boundary conditions are applied in all three directions. The DNS is performed for the case that the Taylor-microscale-based Reynolds number Re_λ is 204, which is sufficiently large to be representative of the wavenumber range relevant for radar observations (Matsuda *et al.*, 2014). The number of grid points is set to 512^3. The Stokes number St, which is defined by the ratio of τ_p to the Kolmogorov time τ_η, is set to 1.0. Nondimensional terminal velocity $S_\mathrm{v} = v_\mathrm{T}/u_\eta$ is one of nondimensional parameters relevant for gravitational settling, where v_T is the terminal velocity given by $\tau_\mathrm{p} g$ and u_η is the Kolmogorov velocity (Wang & Maxey, 1993; Grabowski & Vaillancourt, 1999). In this paper, S_v is set to five values: 0.0, 1.4, 2.7, 6.8 and 11.0.

RADAR REFLECTIVITY FACTOR

The microwave scattering intensity by cloud droplets is proportional to r_p^6, where r_p is the droplet radius, since the scattering is classified as the Rayleigh scattering. Thus, the radar reflectivity factor for the randomly- and uniformly-dispersed droplets Z_random is given by

$$Z_\mathrm{random} = 2^6 r_\mathrm{p}^6 n_\mathrm{p}, \tag{6}$$

where n_p is the droplet number density. For the case of cloud droplets with spatial correlation, Z increases due to the interference between the scattered microwaves. The radar reflectivity factor for monodispersed clustering droplets Z_cluster is given by

$$Z_\mathrm{cluster} = Z_\mathrm{random} + \frac{2^7 \pi^2 r_\mathrm{p}^6}{\kappa^2} E_\mathrm{np}(\kappa), \tag{7}$$

where κ is the absolute value of the difference between the incident and scattered wavenumber vectors $\mathbf{k}_\mathrm{inc}$ and $\mathbf{k}_\mathrm{sca}$: that is $\kappa = |\mathbf{k}_\mathrm{inc} - \mathbf{k}_\mathrm{sca}|$. The power spectrum of droplet number density fluctuations $E_\mathrm{np}(k)$ represents the intensity of clustering for wavenumber k. It should be noted that Eq. (7) assumes isotropic turbulent clustering. $E_\mathrm{np}(k)$ is calculated from the DNS data as

$$E_\mathrm{np}(k) = \frac{1}{\Delta k} \sum_{k-\Delta k/2 \le |\mathbf{k}| < k+\Delta k/2} \widetilde{\Phi}(\mathbf{k}), \tag{8}$$

$$\widetilde{\Phi}(\mathbf{k}) = \frac{1}{L_0^3} \langle \widetilde{n_\mathrm{p}}(\mathbf{k}) \widetilde{n_\mathrm{p}}(-\mathbf{k}) \rangle, \tag{9}$$

where $\widetilde{\Phi}(\mathbf{k})$ is the spectral density function. $\widetilde{n_\mathrm{p}}(\mathbf{k})$ is the Fourier coefficient of the spatial droplet number density distribution $n_\mathrm{p}(\mathbf{x})$, where $n_\mathrm{p}(\mathbf{x})$is given by

$$n_\mathrm{p}(\mathbf{x}) = \sum_{j=1}^{N_\mathrm{p}} \delta(\mathbf{x} - \mathbf{x}_{\mathrm{p},j}), \tag{10}$$

where $\mathbf{x}_{\mathrm{p},j}$ is the position of jth droplet, N_p the total number of droplets, and $\delta(\mathbf{x})$ the Dirac delta function. The detailed equations for calculating $E_\mathrm{np}(k)$ are described in Matsuda *et al.* (2014).

RESULTS AND DISCUSSION

Figure 1 shows the distributions of droplets within the range of $0 < z < 4l_\eta$, where l_η is the Kolmogorov scale, for $S_\mathrm{v} = 0.0$, 2.7, 6.8 and 11.0. Turbulent clustering is clearly observed for all S_v cases. The clustering structure for $S_\mathrm{v} = 2.7$ is similar to that for $S_\mathrm{v} = 0.0$. However, the clusters spread in vertical ($-x$) direction as S_v increases; i.e., the vertical scales of clusters become larger than the horizontal scales. Figure 2 shows the power spectra of droplet number density fluctuations $E_\mathrm{np}(k)$. The horizontal and vertical axes are normalized by using l_η and the average number density, $\langle n_\mathrm{p} \rangle$. The range of the horizontal axis is $0.05 < kl_\eta < 4.0$, which is the relevant wavenumber range for radar observations. As the droplet settling becomes stronger, $E_\mathrm{np}(k)$ increases at small wavenumbers and decreases at large wavenumbers. The increase at small wavenumbers indicates that anisotropies generated by settling lead to large-scale clustering. The decrease at large wavenumbers, on the other hand, indicates that settling weakens small scale clustering (Ayala *et al.*, 2008*b*,*a*; Woittiez *et al.*, 2009).

The power spectra data are used to estimate the increments of Z due to turbulent clustering. This study assumes two types of ideal cloud conditions: (i) a stratocumulus case, where $l_\eta = 1 \times 10^{-3}$ m and (ii) a cumulus case, where $l_\eta = 5 \times 10^{-4}$ m. The corresponding droplet radii are approximately 73 μm and 37 μm, respectively, since $\mathrm{St} = 1.0$. The volume fraction ϕ is set to 10^{-6} for both cases. The microwave frequencies f_m are set to 2.8, 5.3 and 9.4 GHz, which are representative frequencies in typically used frequency bands: S, C and X bands, respectively. Figure 3 shows the estimated increment of Z^dB under the ideal cloud conditions, where Z^dB is the value of Z in units of decibels, defined by $Z^\mathrm{dB}(\mathrm{dBZ}) = 10 \log_{10} Z(\mathrm{mm^6 m^{-3}})$. The increment of Z^dB for the cumulus case is larger than that for the stratocumulus case. This is because the cumulus case contains cloud droplets with smaller size and larger number density than the stratocumulus case since St and ϕ are constant. For both cases, the increment of Z^dB increases in a small amount and then decreases as S_v increases. These

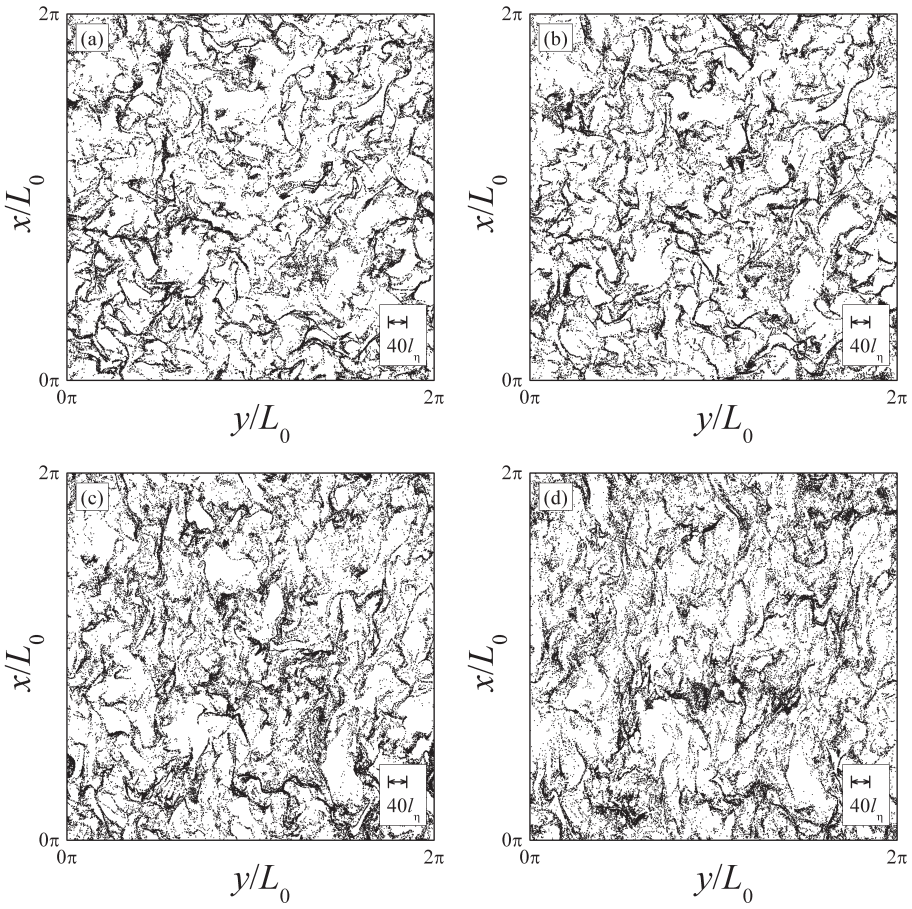

Figure 1. Spatial droplet disstributions in turbulence for (a) $S_v = 0.0$, (b) 2.7, (c) 6.8, and (d) 11.0. Droplets within the range of $0 < z < 4l_\eta$ are drawn, where l_η is the Kolmogorov scale.

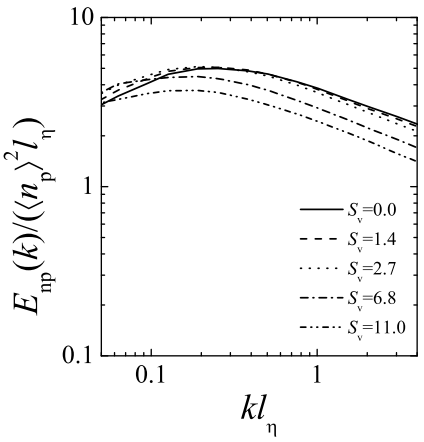

Figure 2. Power spectra of number density fluctuation for turbulent clustering droplets under gravitational settling conditions.

results indicate that the influence of turbulent clustering is suppressed under strong gravitational-settling conditions.

CONCLUSION

This study has been investigated the influence of gravitational settling on the spatial distribution of turbulent clustering droplets and the radar reflectivity factor by means of a three-dimensional direct numerical simulation (DNS) of particle-laden isotropic turbulence. The DNS is conducted for several values of the nondimensional terminal velocity S_v. The spatial droplet distributions obtained by the DNS clearly show the turbulent clustering for all S_v cases. The clusters spread in the settling direction as S_v increases. The power spectrum of droplet number density fluctuations is then calculated from the turbulent clustering data. The results show that the power spectrum increases at small wavenumbers and decreases at large wavenumbers as the droplet settling becomes stronger. The radar reflectivity factor is estimated from the power spectrum under ideal cloud conditions. The results indicate that the influence of turbulent clustering is suppressed under strong gravitational-settling conditions.

REFERENCES

Ayala, O., Rosa, B. & Wang, L.-P. 2008*a* Effects of turbulence on the geometric collision rate of sedimenting droplets. part 2. theory and parameterization. *New J. Phys.* **10**, 075016.

Ayala, O., Rosa, B., Wang, L.-P. & Grabowski, W.W. 2008*b* Effects of turbulence on the geometric collision rate of

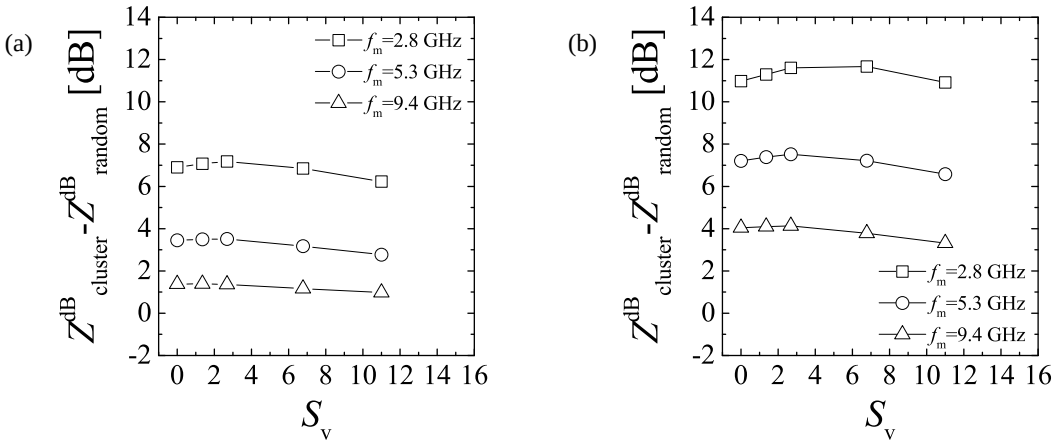

Figure 3. Influence of gravitational settling on the increment of Z^{dB} under ideal cloud conditions; (a) stratocumulus case, where $l_\eta = 1 \times 10^{-3}$ m, (b) cumulus case, where $l_\eta = 5 \times 10^{-4}$ m. The volume fraction ϕ of cloud droplets is 10^{-6}.

sedimenting droplets. part 1. results from direct numerical simulation. *New J. Phys.* **10**, 075015.

Chen, L., Goto, S. & Vassilicos, J.C. 2006 Turbulent clustering of stagnation points and inertial particles. *J. Fluid Mech.* **553**, 143–154.

Erkelens, J.S., Venema, V.K.C., Russchenberg, H.W.J. & Ligthart, L.P. 2001 Coherent scattering of microwave by particles: Evidence from clouds and smoke. *J. Atmos. Sci.* **58**, 1091–1102.

Grabowski, W.W. & Vaillancourt, P. 1999 Comments on "preferential concentration of cloud droplets by turbulence: Effects on the early evolution of cumulus cloud droplet spectra". *J. Atmos. Sci.* **56**, 1433–1436.

Kostinski, A.B. & Jameson, A.R. 2000 On the spatial distribution of cloud particles. *J. Atmos. Sci.* **57**, 901–915.

Matsuda, K., Onishi, R., Hirahara, M., Kurose, R., Takahashi, K. & Komori, S. 2014 Influence of microscale turbulent droplet clustering on radar cloud observations. *J. Atmos. Sci.* **71**, 3569–3582.

Maxey, M.R. 1987 The gravitational settling of aerosol particles in homogeneous turbulence and random flow fields. *J. Fluid Mech.* **174**, 441–465.

Okamoto, H., Nishizawa, T., Takemura, T., Kumagai, H., Kuroiwa, H., Sugimoto, N., Matsui, I., Shimizu, A., Emori, S., Kamei, A. & Nakajima, T. 2007 Vertical cloud structure observed from shipborne radar and lidar: Midlatitude case study during the mr01/k02 cruise of the research vessel mirai. *J. Geophys. Res.* **112**, D08216.

Onishi, R., Baba, Y. & Takahashi, K. 2011 Large-scale forcing with less communication in finite-difference simulations of steady isotropic turbulence. *J. Comput. Phys.* **230**, 4088–4099.

Squires, K.D. & Eaton, J.K. 1991 Preferential concentration of particles by turbulence. *Phys. Fluids A* **3**, 1169–1178.

Stephens, G.L., Vane, D.G., Tanelli, S., Im, E., Durden, S., Rokey, M., Reinke, D., Partain, P., Mace, G.G., Austin, R., L'Ecuyer, T. Haynes, J., Lebsock, M., Suzuki, K., Waliser, D., Wu, D., Kay, J., Gettelman, A., Wang, Z. & Marchand, R. 2008 Cloudsat mission: Performance and early science after the first year of operation. *J. Geophys. Res.* **113**, D00A18.

Wang, L.P. & Maxey, M.R. 1993 Settling velocity and concentration distribution of heavy particles in homogeneous isotropic turbulence. *J. Fluid Mach.* **256**, 27–68.

Woittiez, E.J.P., Jonker, H.J. & Portela, L.M. 2009 On the combined effects of turbulence and gravity on droplet collisions in clouds: A numerical study. *J. Atmos. Sci.* **66**, 1926–1943.